JOURNAL OF GEOPHYSICAL RESEARCH, VOL. 102, NO. C4, PAGES 8663–8679, APRIL 15, 1997

Generation of edge waves in shallow water

T. C. Lippmann

Center for Coastal Studies, Scripps Institution of Oceanography, La Jolla, California

R. A. Holman

College of Ocean and Atmospheric Sciences, Oregon State University, Corvallis

A. J. Bowen

Department of Oceanography, Dalhousie University, Halifax, Nova Scotia, Canada

Abstract. Theoretical growth rates for resonantly driven edge waves in the nearshore are estimated from the forced, shallow water equations of motion for the case of a plane sloping bed. The forcing mechanism arises from spatial and temporal variations in radiation stress gradients induced by a modulating incident wave field. Only the case of exact resonance is considered, where the difference frequencies and wavenumbers satisfy the edge wave dispersion relation (the specific carrier frequencies are not important, only the forced difference values). The forcing is examined in the region seaward of the breakpoint and also within the fluctuating region of surf zone width. In each region, the forcing is dominated by the cross-shore gradient of onshore directed momentum flux, except for large angles of incidence and the lowest edge wave modes. Outside the surf zone, the spatial and temporal variation of the forcing is determined by considering the interaction of two progressive shallow water waves approaching the beach obliquely. In the surf zone, incident wave amplitudes are assumed to be proportional to the water depth. Thus inside the breakpoint, radiation stress gradients are constant and no forcing occurs. However, at the breakpoint, gradients arising from breaking and nonbreaking waves are turned on and off (like a wave maker) with timescales and length scales determined by the modulation of the breaker position. The forcing in this region is stronger, with inviscid growth rates resulting in edge waves growing to the size of the incident waves of the order of about 10 edge wave periods, a factor of 2-10 times larger than in the offshore region. Using a simple parameterization for frictional damping, edge wave equilibrium amplitudes are found to depend linearly on the ratio $\tan\beta/C_d$, where β is the beach slope and C_d is a bottom drag coefficient. For $\tan\beta/C_d$ about 3-10, equilibrium amplitudes can be as much as 75% of the incident waves over most of the infragravity portion of the spectrum. When the forcing is turned off, these dissipation rates result in a half-life decay timescale of the order of 10-30 edge wave periods.

Introduction

Since the initial observations of *Munk* [1949] and *Tucker* [1950] much effort has been aimed at understanding the origin and importance of low-frequency (relative to wind waves) surface gravity waves in shallow water. Field data obtained on natural beaches have shown that long-period ($O(10^2$-10^3 s)) infragravity motions often dominate power spectra in the inner surf zone and swash, particularly during storms when incident wave heights in shallow water are severely limited by breaking [*Huntley*, 1976; *Huntley et al.*, 1981; *Holman*, 1981; *Thornton and Guza*, 1982; *Holman and Sallenger*, 1985; *Sallenger and Holman*, 1987]. The data also indicate that infragravity surface gravity waves are predominantly composed of edge waves, longshore progressive waves trapped to the shoreline by refraction, together with a smaller component of leaky waves, normally reflected waves which escape from the nearshore into deep water [*Guza and Thornton*, 1985; *Oltman-Shay and Guza*, 1987; *Howd et al.*, 1991; *Herbers et al.*, 1995b].

The existence of edge waves in nature has been known for some time. *Bowen and Guza* [1978] and *Holman* [1981] suggest that the growth of edge wave amplitudes, a_n, is determined by the coupling between the nonlinear forcing, $\mathbf{F}(a_1, a_2, x)$, arising from an interacting incident wave field and the cross-shore edge wave waveform, $\phi_n(x)$,

$$\frac{\partial a_n}{\partial t} \sim \frac{\sigma_e}{g}\int_0^\infty \mathbf{F}(a_1,a_2,x)\phi_n(x)dx \qquad (1)$$

where a_1 and a_2 are incident wave amplitudes, σ_e is the edge wave radian frequency, g is gravity, t is time, and x is the cross-shore coordinate. Growth occurs when the forcing pattern is not orthogonal to the edge wave waveform. The details of the forcing are described by the spatially varying form of $\mathbf{F}$. In this work we derive an analytic expression for $\mathbf{F}$ and numerically integrate the coupling integral to obtain an estimate for the growth rate.

The principal forcing is believed to be derived from pairs of incident wind waves, which produce spatial and temporal

Paper number 96JC03722.
0148-0227/97/96JC-03722$09.00

variations in radiation stress gradients of the same timescale and length scale as the edge waves. Outside the surf zone in intermediate and shallow depths, forcing occurs through a typical second-order nonlinear interaction [*Gallagher*, 1971; *Bowen and Guza*, 1978]. Inside the surf zone, difficulties arise in specifying the forcing functions all the way to the shoreline. Here we assume that amplitude variations are eliminated by saturation and no oscillatory forcing occurs. However, there is a time dependent momentum flux induced by the modulation in breakpoint position associated with the variation in incident wave height [*Foda and Mei*, 1981; *Symonds et al.*, 1982; *Symonds and Bowen*, 1984; *Schaffer*, 1993].

Outside the surf zone (referred to herein as offshore forcing) the generation mechanism evolves from the second-order forced (or bound) wave generated by wave groups in intermediate water depths [*Biesel*, 1952; *Longuet-Higgins and Stewart*, 1962, 1964; *Hasselmann*, 1962]. In two dimensions, the bound wave is, in principal, released at breaking and reflected at the shoreline; thus the incoming and outgoing waves form a complex pattern in the cross-shore, however, without the longshore component necessary for edge wave generation. This idea was extended to three dimensions by *Gallagher* [1971], who showed that nonlinear interactions between incident wave pairs could produce low-frequency oscillations with a nonzero alongshore wavenumber. *Bowen and Guza* [1978] generalized Gallagher's model to include forcing of all modes and showed with laboratory experiments that resonant response was greater than forced response. This same conclusion was reached by *Foda and Mei* [1981] in a fourth-order WKB expansion of the momentum equations.

In the surf zone, forcing occurs because an interacting incident wave field produces spatial and temporal variations in locations of the position at which a wave breaks (herein referred to as surf zone forcing). Momentum is transferred from incident to lower frequencies through wave breaking, and the interactions again lead to fluctuations in the flow field with timescales and space scales of the order of wave groups. This idea was first explored as a generating mechanism for long waves by *Foda and Mei* [1981] and *Symonds et al.* [1982]. As will be shown later, there is also a contribution from nonbreaking waves within the region of fluctuating surf zone width.

In the work by *Foda and Mei* [1981], low-frequency waves are generated by wave-wave interaction assuming a fixed breakpoint position for all waves. This allows incident modulations to progress to the shoreline, and edge waves are forced everywhere. In nature, however, the initial breakpoint of individual waves is not constant through time, nor is the breaker line uniform along the beach. Under most conditions, temporal and spatial variations in the width of the surf zone occur on large timescales and space scales, of the order of infragravity scaling [*Symonds et al.*, 1982]. Although the basic physics inshore from the breakpoint is doubtful, Foda and Mei do consider resonant edge wave growth, also considered here, and thus a brief comparison with their results is made later.

Symonds et al. [1982] consider the problem of long wave forcing by time modulations in surf zone width for the case of a plane sloping bed and later included interactions with barred topography [*Symonds and Bowen*, 1984]. In contrast to *Foda and Mei* [1981], they assume constant breaking criteria so that modulations in incident wave heights are manifested in fluctuations in the width of the surf zone. However, their model is limited to only two dimensions (no inclusion of longshore variability), precluding the possibility of edge wave forcing. Nevertheless, the results of Symonds et al. suggest that edge wave generation by temporal variations in surf zone width is possible.

Schaffer and Svendsen [1988] retain the ideas of *Foda and Mei* [1981] and *Symonds et al.* [1982], by allowing fluctuations in both breakpoint positions and incident wave energy inside the breakpoint, although they limit their discussion to the two-dimensional case. *List* [1992] extends this mechanism in a numerical model to include arbitrary topography and further includes incoming bound waves, crudely modeled empirically using field data, as do *Schaffer and Svendsen* [1988]. They forego a more theoretical approach since it is not clear what the correct boundary conditions are for bound wave dynamics in the shoaling and breaking region, although it is expected the forced motions become nearly resonant in shallow water [*Longuet-Higgins and Stewart*, 1964; *Okihiro et al.*, 1992].

Schaffer [1994] uses a WKB (optics) approach to describe the incident waves and drives the edge waves with radiation stress modulations determined by fluctuating amplitudes (i.e., the two incident waves are assumed to approach from the same direction). Numerical solutions are considerably complicated by an angular bottom which necessitates a matching condition at a corner in the profile. Furthermore, Schaffer's offshore profile is horizontal; thus waves propagating offshore beyond this "shelf" are no longer refracted, thus limiting the possible edge waves which can exist. Low-frequency response is found through numerical calculation, with resonant modes determined critically by the single-incident wave angle and the offshore profile configuration. This results in a very specific set of results only valid for these restricted set of conditions.

In this paper we present a mechanism for the resonant forcing of edge waves in shallow water through modulations in radiation stress gradients. We consider two interacting shallow water incident waves whose difference wavenumbers and frequencies satisfy the edge wave dispersion relation. The total forcing is found by integrating the growth rate equation from the shoreline to deep water (relative to wind waves). Contributions to the forcing from inside and outside the surf zone are examined by separating the forcing integral at the breakpoint. We consider the simplest case of a planar beach profile, where forcing in the surf zone is determined by a time and space dependent fluctuation in the width of the surf zone.

In the next section we review the theory for edge waves on a plane sloping beach beginning with the forced shallow water (depth integrated), linearized equations of motion, leading to an analytic expression for the initial (undamped) edge wave growth rate. Model results are then presented, comparing the relative contributions to the forcing from the components of the radiation stress and also the strength of inviscid growth rates in the surf zone and offshore regions. Results are then discussed in terms of the validity of model assumptions, parameter sensitivity, and implications in field situations (spectral forcing). The effect of a linearized dissipation term on edge wave growth is discussed. In Appendix B the extension of the calculations to an incident wave spectrum is briefly discussed.

Model

Edge Wave Theory

The forced, shallow water (depth integrated), linearized equations of motion including a linearized dissipation term are [*Phillips*, 1977]

$$\frac{\partial u}{\partial t}+g\frac{\partial \eta}{\partial x}=-\frac{1}{\rho h}\left[\frac{\partial}{\partial x}S_{xx}+\frac{\partial}{\partial y}S_{xy}\right]-\lambda u \tag{2}$$

$$\frac{\partial v}{\partial t}+g\frac{\partial \eta}{\partial y}=-\frac{1}{\rho h}\left[\frac{\partial}{\partial x}S_{xy}+\frac{\partial}{\partial y}S_{yy}\right]-\lambda v \tag{3}$$

and the continuity equation

$$\frac{\partial \eta}{\partial t}+\frac{\partial}{\partial x}(hu)+\frac{\partial}{\partial y}(hv)=0 \tag{4}$$

where x and y are the cross-shore and alongshore horizontal Cartesian coordinates with x positive seaward (for a right-hand system with z positive upward), u and v are the corresponding horizontal components of velocity, η is sea surface elevation, λ is a friction coefficient (discussed later), h is the still water depth, and ρ is the density of water. The equations have been averaged over an incident wave period so that the time dependence is on infragravity and longer scales. S_{pq} are the radiation stresses of short (incident) waves introduced by *Longuet-Higgins and Stewart* [1962, 1964] and describe the flux of pth directed momentum in the qth direction.

Combining (2)-(4) and temporarily dropping the damping term yield a single second-order (inviscid) equation in sea surface elevation [*Mei and Benmoussa*, 1984],

$$\begin{aligned}&\frac{\partial^2 \eta}{\partial t^2}-g\frac{\partial}{\partial x}\left(h\frac{\partial \eta}{\partial x}\right)-g\frac{\partial}{\partial y}\left(h\frac{\partial \eta}{\partial y}\right)\\&\quad=-\frac{1}{\rho}\left[\frac{\partial}{\partial x}\left(\frac{\partial S_{xx}}{\partial x}+\frac{\partial S_{yx}}{\partial y}\right)+\frac{\partial}{\partial y}\left(\frac{\partial S_{xy}}{\partial x}+\frac{\partial S_{yy}}{\partial y}\right)\right]\\&\quad=F_{xx}+F_{yx}+F_{xy}+F_{yy}=\mathbf{F}\end{aligned} \tag{5}$$

where F_{xx}, F_{yx}, F_{xy}, and F_{yy} are the components of the total forcing, $\mathbf{F}$, corresponding to the four second derivatives on the right-hand side. The forcing and frictional dissipation are assumed to be of second order, and we ignore their effects on both the wave solutions and the dispersion relation (which could be significant if the forcing and friction are large).

For a plane beach, $h=x\tan\beta$, where β is the beach slope, the homogenous case (free waves) is satisfied by edge waves of the form [*Eckart*, 1951]

$$\eta_n(x,y,t)=\tfrac{1}{2}a_n\phi_n(x)e^{-i(k_e y-\sigma_e t)}+(*) \tag{6}$$

where $\sigma_e=2\pi f_e$ and $k_e=2\pi/L_e$ are the edge wave radian frequency and alongshore wavenumber (f_e and L_e are the edge wave frequency and wavelength), n is the edge wave mode number, a_n are the complex modal amplitudes (which can be resolved into a magnitude and phase), (*) indicates the complex conjugate of the previous term, and $i=\sqrt{-1}$. The cross-shore structure of the edge wave waveform, $\phi_n(x)$, is given by

$$\phi_n(x)=e^{-k_e x}L_n(2k_e x) \tag{7}$$

where L_n is the Laguerre polynomial of order n. The approximate shallow water edge wave dispersion relation is given by [*Eckart*, 1951]

$$\sigma_e^2=gk_e(2n+1)\tan\beta \tag{8}$$

Growth Rates

We seek an expression for the time rate of change of edge wave modal amplitudes, or growth rate, $\partial a_n/\partial t$. Substituting (6) into (5) and allowing a_n to be a slowly varying function of time give

$$\left[\frac{\partial^2 a_n}{\partial t^2}\phi_n+i2\sigma_e\frac{\partial a_n}{\partial t}\phi_n-a_n Z(\phi_n)\right]e^{-i\psi_e}=\mathbf{F} \tag{9}$$

where

$$Z(\phi_n)=g\frac{\partial}{\partial x}\left(h\frac{\partial \phi_n}{\partial x}\right)+\left(\sigma_e^2-ghk_e^2\right)\phi_n$$

$$\psi_e=k_e y-\sigma_e t.$$

In (9), and in subsequent equations for the growth rate, we have dropped the complex conjugate for brevity, thus later we will take the real part to obtain the magnitude and phase. The function $Z(\phi_n)$ is the homogeneous equation for shallow water waves and vanishes for the case of resonance considered here. If we assume that the edge wave growth rate is slow relative to its period, then the first term describing the acceleration in growth can be neglected. Thus an equation for the initial edge wave growth rate is

$$i2\sigma_e\frac{\partial a_n}{\partial t}\phi_n e^{-i\psi_e}=\mathbf{F} \tag{10}$$

The cross-shore dependence is eliminated by multiplying by ϕ_n and integrating from the shoreline to infinity in the cross-shore direction, as in (1). Incorporating the dispersion relation and dividing by the primary incident wave amplitude (described later), $(a_i)_o$, the normalized growth rate becomes

$$\frac{1}{(a_i)_o f_e}\frac{\partial a_n}{\partial t}e^{-i\psi_e}=\frac{-2\pi i}{(a_i)_o g\tan\beta(2n+1)}\int_0^\infty \mathbf{F}\phi_n dx \tag{11}$$

in which the normalizing factor $\int_0^\infty \phi_n^2 dx=1/2k_e$ has been used. The coupling integral expresses the rate at which energy is transferred from the incident waves to resonant lower-frequency motions. The inverse of the magnitude of (11) is the number of edge wave periods necessary for the edge wave to grow to the size of the primary incident wave.

Coupling Integral and Incident Wave Amplitudes

In deep water, resonant interactions are quartic and only forced waves are produced by triad interactions. In shallower water, resonant triad interactions can occur, producing variation in radiation stress which can match the edge wave dispersion relation. This spatial and temporal modulation gives rise to the possibility of edge wave growth. Although the modulation scales remain the same, the forcing function $\mathbf{F}$, which depends on wave amplitude, varies as waves shoal in intermediate water and eventually break in the surf zone. As a consequence, there are two distinct forcing regions separated by the contour of the breaker line, $x_b(y,t)$ (shown graphically in Figure 1), and the coupling integral can be written

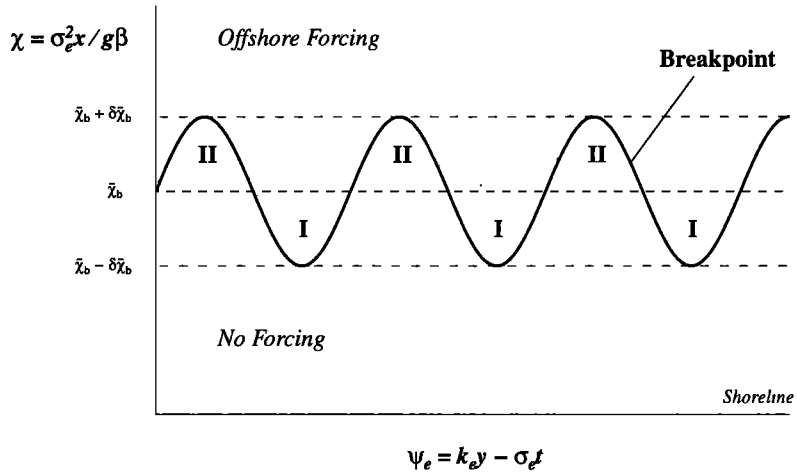

Figure 1. Graphical representation of the edge wave forcing regions relative to an oscillating breaker line. The vertical axis is $\chi = \sigma_e{}^2 x/g\tan\beta$ and the horizontal axis is $\psi_e = k_e y - \sigma_e t$. The offshore forcing region is defined as seaward of the most seaward breakpoint. Inside the minimum breakpoint, no forcing occurs. The range of forcing by a modulating breakpoint position is a function of incident wave modulation, δ. The regions where waves are alternately shoaling and breaking (between $\bar{\chi}_b$ and the oscillating breaker line) are labeled I and II, respectively.

$$\int_0^\infty \mathbf{F}(a_1,a_2,x)\phi_n(x)dx = \int_0^{x_b(y,t)} \mathbf{F}_{sz}(a_1,a_2,x)\phi_n(x)dx + \int_{x_b(y,t)}^\infty \mathbf{F}_{off}(a_1,a_2,x)\phi_n(x)dx \quad (12)$$

where $\mathbf{F}_{sz}$ and $\mathbf{F}_{off}$ are the forcing inside and outside the breakpoint, respectively. The forcing functions are determined by the temporal fluctuations of radiation stress gradients, which are in turn determined by modulations in incident wave amplitude.

It is the slowly varying breaker line, $x_b(y,t)$, that creates first-order fluctuations in the surf zone coupling integral. If we assume that the breakpoint varies sinusoidally with ψ_e time and length scales (described later) and further separate the coupling integral at $\bar{x}_b$ and expand in a Taylor's series about $\bar{x}_b$, then to first order, (12) can be written (Appendix A)

$$\int_0^\infty \mathbf{F}\phi_n dx = \delta\bar{x}_b \cos\psi_e \phi_n(\bar{x}_b)\left[\mathbf{F}_{sz}(a_1 a_1,\bar{x}_b) - \mathbf{F}_{off}(a_1 a_1,\bar{x}_b)\right] + \int_{\bar{x}_b}^\infty F_{off}(a_1 a_2,x)\phi_n(x)dx \quad (13)$$

Thus the first-order contributions to edge wave growth occur through primary interactions from both breaking and nonbreaking waves within the fluctuating region of surf zone width and through cross-interactions of a pair of waves seaward of the average breakpoint position.

In the following, the wave field is considered to be composed of two waves, a primary wave with amplitude a_1 and longshore wavenumber and frequency (k_1, f_1) and a secondary wave with amplitude a_2 and slightly different wavenumber and frequency (k_2, f_2). If we choose

$$a_2 = \delta a_1 \quad (14)$$

where $\delta << 1$ is a constant, then the primary wave determines the mean wave amplitude and the modulation (about the mean) is determined from a_2 [*Symonds et al.*, 1982].

Because of sharp differences in the shoaling and breaking regions, the amplitudes of the incident waves are treated differently. In the offshore region the amplitudes are described by progressive shallow water waves over a plane sloping bottom; thus an interacting wave field has modulations all the way to the breakpoint. Wave amplitudes in this region are referenced to a convenient location (e.g., the breakpoint). Inside the surf zone, wave amplitudes are strongly attenuated shoreward by breaking and are described as a linear function of local depth,

$$a_i = \tfrac{1}{2}\gamma h \qquad x < x_b \quad (15)$$

where γ is a constant of $O(1)$ [e.g., *Thornton and Guza*, 1982]. For a plane beach, reference amplitudes can then be given by

$$(a_i)_o = \tfrac{1}{2}\gamma x_b \tan\beta \quad (16)$$

where x_b is the position of the breaker line, a function of y and t.

Once the incident waves break, modulations in incident amplitudes vanish and the forcing becomes constant shoreward. The possibility for edge wave forcing occurs because the breakpoint position varies on timescales and space scales associated with the incident beat. Thus the limits of integration in (12) for the surf zone integral will have modulations with edge wave timescales and space scales that are determined by the fluctuating breakpoint position (Figure 2). The magnitude of the modulation is determined by the maximum and minimum breakpoint amplitudes, $a_{max} = a_1 + \delta a_1$ and $a_{min} = a_1 - \delta a_1$, respectively, so that the cross-shore range over which forcing occurs is defined by

$$\bar{x}_b - \delta\bar{x}_b \le x_b \le \bar{x}_b + \delta\bar{x}_b \quad (17)$$

where $\bar{x}_b$ is the mean breaker position.

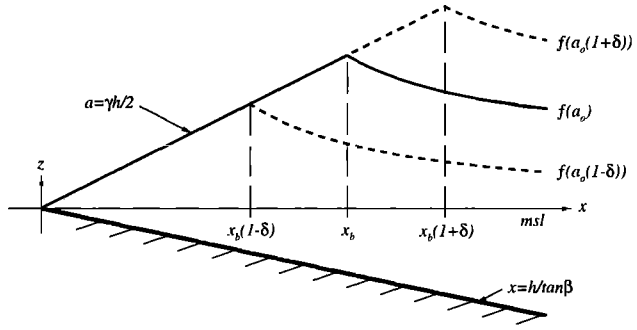

Figure 2. Graphical representation of the envelop of incident wave amplitudes over a plane sloping bed as a function of cross-shore distance. Surf similarity ($a=\gamma h/2$) is assumed once waves are breaking so that modulations in incident amplitudes produce variations in surf zone width. The vertical (elevation) and horizontal (cross-shore distance) dimensions are arbitrary.

Parameterizing the Forcing

Following *Phillips* [1977], the general form of the radiation stress is given by

$$S_{pq}=\rho\int_{-h}^{\bar{\eta}}\overline{\frac{\partial\Phi}{\partial x_p}\frac{\partial\Phi}{\partial x_q}}dz+\delta_{pq}\left[\int_{-h}^{\bar{\eta}}\bar{p}dz-\tfrac{1}{2}\rho g\left(h+\bar{\eta}\right)^2+\tfrac{1}{2}\rho g\overline{\eta^2}\right] \tag{18}$$

where $\mathbf{x}$ is the horizontal space vector in which subscripts p and q denote either horizontal coordinate, Φ is the velocity potential of the incident waves, $\bar{p}$ is the mean pressure, and δ_{pq} is the Kronecker delta. The momentum balance has been spatially averaged in the direction of the wave crests (allowing separation of the turbulent and wave terms) and temporally averaged over the incident wave period (allowing mean or slowly varying properties to be evaluated), denoted with the overbars in (18). In shallow water $\bar{p}=-\rho gz$ and assuming $\bar{\eta}\approx 0$ at second order,

$$S_{pq}\approx\rho h\overline{\frac{\partial\Phi}{\partial x_p}\frac{\partial\Phi}{\partial x_q}}+\delta_{pq}\frac{\rho}{2g}\overline{\left(\frac{\partial\Phi}{\partial t}\right)^2} \tag{19}$$

We consider the bichromatic case where the incident wave field is composed of two discrete wave trains with slightly different wavenumber and frequency,

$$\Phi=\Phi_1+\Phi_2 \tag{20}$$

where the subscripts 1 and 2 refer to the two incident waves. Substituting Φ into (19) produces

$$S_{pq}=S_{pq}\left(\Phi_1\Phi_1\right)+2S_{pq}\left(\Phi_1\Phi_2\right)+S_{pq}\left(\Phi_2\Phi_2\right) \tag{21}$$

The first and last terms represent the self-self interactions which generate mean flows and harmonics. The harmonics do not contribute to low-frequency forcing in either region and are therefore neglected. Letting the amplitude of a primary wave Φ_1 be much larger than any secondary waves Φ_2 (equation (14)), then $\Phi_1\Phi_1$ terms are of $O(1)$, while cross-interaction terms $\Phi_1\Phi_2$ are $O(\delta)$ and $\Phi_2\Phi_2$ terms are $O(\delta^2)$. The stress arising from $\Phi_i\Phi_i$ interactions will generate a set-down outside the breakpoint and a setup inside the breakpoint within the fluctuating region of the surf zone, which will oscillate at the same frequency and wavenumber as the fluctuating surf zone boundary (given by the time varying contour of the breaker line).

We choose the velocity potential for progressive shallow water waves over a plane sloping bottom after *Stoker* [1947]

$$\Phi_i=\frac{a_i g}{\sigma_i}\left[J_o\left(X_i\right)\cos\psi_i+Y_o\left(X_i\right)\sin\psi_i\right] \tag{22}$$

where

$$X_i=2\left(\frac{\sigma_i^2 x}{g\tan\beta}\right)^{1/2}$$

$$\psi_i=\left(k_i y-\sigma_i t\right)$$

and J_o and Y_o are the zero-order bessel functions of the first and second kind, respectively, k_i is the alongshore component of the incident wavenumber vector, and the subscript i is an index which refers to individual incident waves. For $X_i>3$ (equivalent to $H>\sim(T\tan\beta)^2/2$, so valid for nearly all oceanic cases), the bessel functions may be approximated by [*Stoker*, 1947]

$$J_o\left(X_i\right)\approx\left(\frac{2}{\pi X_i}\right)^{1/2}\cos\left(X_i-\frac{\pi}{4}\right) \tag{23a}$$

$$Y_o\left(X_i\right)\approx\left(\frac{2}{\pi X_i}\right)^{1/2}\sin\left(X_i-\frac{\pi}{4}\right) \tag{23b}$$

Introducing complex notation yields the following form for Φ_i

$$\Phi_i=\tfrac{1}{2}\frac{a_i g}{\sigma_i}\left(\frac{2}{\pi X_i}\right)^{1/2}e^{i\left(X_i-\psi_i+\frac{\pi}{4}\right)}+(*) \tag{24}$$

The form of our velocity potential is only strictly valid for waves approaching the beach shore normally. However, *Guza and Bowen* [1975] show that nonnormal angles of incidence have only small effects on the form of the velocity potential due to refraction decreasing the angle of incidence and show that where shallow water solutions are valid, the solutions for shore-normal and oblique incidence angle are nearly the same.

Substitution of (24) into (21) produces terms with sum and difference wavenumbers and frequencies. The sum terms (high-frequency forced waves) are unimportant to the generation of infragravity motions [*Bowen and Guza*, 1978] and are not considered further. The difference terms describe the long timescales and space scales of the incident wave modulation and allow for the possibility for edge waves at infragravity frequencies

$$\sigma_f=\sigma_1-\sigma_2 \tag{25a}$$

and

$$\left|k_f\right|=\left|k_1-k_2\right| \tag{25b}$$

where k_1 and k_2 are the longshore wavenumbers of the incident waves and the subscript f indicates the forced difference values associated with the incident wave modulation. For resonance to occur, (25a) and (25b) must satisfy the edge wave dispersion relation (8).

Incident wave angles are assumed to follow Snell's law for wave refraction and are chosen at the breakpoint where the

linear shallow water phase velocity is simply a function of the local depth, $c=\sqrt{gh}$, so that

$$k_i=\frac{\sigma_i^2}{g}\sin\alpha_\infty=\frac{\sigma_i}{\sqrt{gh_o}}\sin(\alpha_i)_o \tag{26}$$

where ∞ indicates the deep water condition and $(\alpha_i)_o$ are the wave angles of the individual waves taken at some reference depth, h_o. If we further reference a_i to the breakpoint, where $h_o=h_b$, then products a_1a_2 are given from (24) by

$$a_1a_2=\frac{\pi}{2}(a_1)_o(a_2)_o\left[(X_1)_o(X_2)_o\right]^{1/2} \tag{27}$$

where the subscript o refers to values at the reference position (e.g., the breakpoint).

Now substituting (24) into (19), incorporating (26)-(27), and evaluating the appropriate derivatives give an analytic form of the radiation stress

$$S_{pq}=\frac{A_o}{X_e}\left\{I_{pq}+\delta e^{i(x_e-\psi_e)}\left(J_{pq}-iK_{pq}\right)+O(\delta^2)\right\} \tag{28}$$

where

$$A_o=\frac{\rho g}{2}(a_1)_o{}^2(X_e)_o$$

$$I_{pq}=\begin{vmatrix}3 & 2\alpha_1\\ 2\alpha_1 & 2\alpha_1{}^2+1\end{vmatrix}$$

$$J_{pq}=\begin{vmatrix}3+\frac{1}{2}\Lambda & \alpha_1+\alpha_2\\ \alpha_1+\alpha_2 & 2\alpha_1\alpha_2+1\end{vmatrix}$$

$$K_{pq}=\begin{vmatrix}X_e\Lambda & \frac{\Lambda}{2}(X_1\alpha_1-X_2\alpha_2)\\ \frac{\Lambda}{2}(X_1\alpha_1-X_2\alpha_2) & 0\end{vmatrix}$$

$$\Lambda=\frac{1}{X_1X_2}$$

$$X_e=2\left(\frac{\sigma_e{}^2x}{g\tan\beta}\right)^{1/2}$$

and $\sin(\alpha_1)_o$ and $\sin(\alpha_2)_o$ have been abbreviated α_1 and α_2, respectively, for simplicity. In (28), $O(1)$ terms are a result of $\Phi_1\Phi_1$ interactions, $O(\delta)$ terms are from $\Phi_1\Phi_2$ interactions, and $O(\delta^2)$ terms are from $\Phi_2\Phi_2$ interactions.

Using typical values found in nature, $f_1\approx f_2\approx 0.1$ Hz, $x_b\approx 100$ m, and $\tan\beta\approx 0.02$, we find Λ is $O(10^{-3})$ at the breakpoint, and therefore terms in (28) containing Λ contribute negligibly to the interaction and are neglected in the following. This implies that although interactions of the incident waves determine the response frequency, the specific carrier frequencies are not important.

Response Outside the Surf Zone

The forcing function outside the mean breakpoint position is found directly by inserting terms of order δ in (28) (arising from cross-interaction radiation stresses) into the right-hand side of (5) and evaluating the second spatial derivatives,

$$\mathbf{F}_{off}=\frac{12A_o}{\rho}\left(\frac{\sigma_e^2}{g\tan\beta}\right)^2\delta e^{i(X_e-\psi_e)}$$

$$\cdot\left(\frac{3-X_e^2-i3X_e}{X_e^5}+\frac{\sin\alpha_1+\sin\alpha_2}{3(2n+1)X_e^2}-\frac{2\sin\alpha_1\sin\alpha_2+1}{12(2n+1)^2X_e}\right) \tag{29}$$

The three terms are derived from the components of the interaction radiation stress from F_{xx}, $2F_{xy}$, and F_{yy}. The three components of the interaction forcing are compared later. Contributions to edge wave forcing by nonbreaking waves seaward of the breakpoint but within the fluctuating region of surf zone width are considered in the next section.

Inserting (29) into the coupling integral in (13) results in a complex expression for the undamped response of edge waves by oscillating forcing seaward of the mean breakpoint. After taking the real part, expressions for the normalized initial growth rate magnitude, G_{off}, and phase, θ_{off}, are given by

$$G_{off}=\frac{1}{f_e(a_1)_o}\frac{\partial a_n}{\partial t}=\frac{3\pi\gamma}{4(2n+1)}\delta(\overline{X_b})^3\left(P_n^2+Q_n^2\right)^{1/2} \tag{30}$$

$$\theta_{off}=\arctan\left(\frac{Q_n}{P_n}\right)$$

where

$$P_n=\int_{\overline{X_b}}^{\infty}(B_2\cos X_e-B_1\sin X_e)\phi_nX_e\,dX_e$$

$$Q_n=\int_{\overline{X_b}}^{\infty}(B_1\cos X_e+B_2\sin X_e)\phi_nX_e\,dX_e$$

$$B_1=\frac{3-X_e{}^2}{X_e{}^5}+\frac{\sin\alpha_1+\sin\alpha_2}{3(2n+1)X_e{}^2}-\frac{2\sin\alpha_1\sin\alpha_2+1}{12(2n+1)^2X_e}$$

$$B_2=\frac{3}{X_e{}^4}$$

Surf Zone Response From Breaking and Nonbreaking Waves

The cross-shore integral parameterizing the surf zone contribution to the total edge wave forcing ranges from the shoreline to the breakpoint, $0\le x\le x_b$. Following *Symonds et al.* [1982], we do not allow modulations in wave amplitude inside the minimum, most shoreward breakpoint by choosing γ to be constant for all waves. Thus for a plane beach, modulations in breakpoint amplitudes generate spatial and temporal variations in the width of the surf zone. Symonds et al. used this as the basis for their two-dimensional long wave model.

Wave amplitudes are expressed in terms of cross-shore breakpoint position using (16). The surf zone forcing function is then found by inserting (28) into the right-hand side of (5) and evaluating the spatial derivatives. Since we are only interested in first-order approximation, we need only retain the primary self-interaction terms (Appendix A). Inside the breakpoint first-order radiation, stress gradients for breaking and nonbreaking waves are given by

$$\frac{\partial S_{xx}}{\partial x} = 6B_o x\Big|_{\text{breaking}} - \frac{3B_o \bar{x}_b (X_e)_o^3}{2X_e}\Bigg|_{\text{nonbreaking}} \tag{31a}$$

$$\frac{\partial S_{yx}}{\partial y} = 0 \tag{31b}$$

$$\frac{\partial S_{xy}}{\partial x} = 4B_o x \sin\alpha_1\Big|_{\text{breaking}} \tag{31c}$$

$$\frac{\partial S_{yy}}{\partial y} = 0 \tag{31d}$$

where $B_o = \rho g(\gamma\tan\beta)^2/8$. The dependence of wave angle on depth is eliminated using (26) (the incident alongshore wavenumber is conserved across the nearshore region).

Since we are taking γ to be constant, all modulations inside the initial breakpoint vanish, and each component of (31) is constant. In essence, variations in the forcing are defined by a wave maker type problem, where the forcing is turned on and off at the initial breakpoint (as in the work by *Symonds et al.* [1982]). Periodic fluctuations in radiation stress gradients arise from fluctuations in the position of the initial breakpoint on timescales and space scales of the modulation. Alongshore modulations allow for the possibility of edge waves.

Because radiation stress gradients are discontinuous at the breakpoint, we represent (31) as a complex Fourier Series. Extending *Symonds et al.* [1982],

$$\left.\frac{\partial S_{pq}}{\partial x_p}\right|_{x=x_b} = C_o + \sum_{m=1}^{\infty} C_m e^{im\psi'} + (*) \tag{32}$$

where

$$C_m = \frac{1}{2L}\int_{\tau_1(y,t)}^{\tau_2(y,t)} \frac{\partial S_{pq}}{\partial x_p} e^{-im\psi'}\, d\psi'$$

where τ_1 and τ_2 define the interval over which forcing occurs and (*) indicates the complex conjugate of the previous terms under the summation. The form of (32) is given for the breaking waves only; nonbreaking waves in the fluctuating region of surf zone width are π out of phase with (32). Symonds et al. present an extensive discussion for finding the Fourier limits of integration for the two-dimensional case. We extend their ideas to three dimensions in the following. The mean breakpoint amplitude is defined by the larger wave, and the fluctuation about the mean is defined by the amplitude modulation, δ, such that by using linear superposition of two sinusoidal waves

$$a_b = a_1\left[1 + \delta\cos\left(\frac{1}{2}\overline{X_b} - \psi_e\right)\right] \tag{33}$$

where $\overline{X_b}$ is the mean X_e value corresponding to $x = \bar{x}_b$. We can express (33) in terms of breakpoint positions using (16)

$$x_b = \bar{x}_b\left[1 + \delta\cos\left(\frac{1}{2}\overline{X_b} - \psi_e\right)\right] \tag{34}$$

where $\bar{x}_b$ is the mean breakpoint position. The upper limit of integration in (32) is determined from the argument of (34)

$$\tau_2 = \left|\frac{1}{2}\overline{X_b} - \psi_e\right| = \cos^{-1}\left(\frac{x_b - \bar{x}_b}{\delta\bar{x}_b}\right) \tag{35}$$

Symonds et al. [1982] show that for small δ the limits of integration are symmetric; hence $\tau_1 = -\tau_2 \equiv \tau$. Using (35), the Fourier coefficients are

$$C_o = \text{const} \tag{36a}$$

$$C_m = \frac{\partial S_{pq}}{\partial p}\frac{\sin m\tau}{m\tau} \qquad m = 1, 2, \ldots \tag{36b}$$

The first term in the series (C_o) represents the mean value over all ψ_e space and subsequently vanishes when second derivatives are taken. For $m > 0$, the series consists of a primary modulation ($m = 1$) and its harmonics ($m > 1$). Thus to lowest order (considering only forcing contributions from the primary) the total forcing from breaking and nonbreaking waves in the fluctuating region of surf zone width is found (after evaluating the second spatial derivatives)

$$\mathbf{F}_{sz} = \frac{-12B_o}{\rho} e^{i\left(\frac{1}{2}\overline{X_b} - \psi_e\right)} \cdot\left\{\left(1 + \frac{3}{8}\right)\frac{\sin\tau}{\tau} - \frac{\sin\alpha_1 X_b^2}{6(2n+1)}\left(\frac{\cos\tau}{\tau} - \frac{\sin\tau}{\tau^2} + i\frac{\sin\tau}{\tau}\right)\right\} \tag{37}$$

The first and second terms arise from F_{xx} forcing by breaking and nonbreaking waves, respectively. The remaining three terms arise from F_{xy} forcing by breaking waves only. The components of the forcing are compared later.

The initial growth rate is found by inserting (37) into the first coupling integral and evaluating in the same manner as in the offshore region, except that the limits of integration are now given by (17). Taking the real part gives expressions for the magnitude, G_{sz}, and phase, θ_{sz}, of the initial edge wave growth rate in the fluctuating region of surf zone width

$$G_{sz} = \frac{1}{f_e(a_1)_o}\frac{\partial a_n}{\partial t} = \frac{12\gamma}{(2n+1)\overline{X_b}^2}\left(M_n^2 + N_n^2\right)^{1/2} \tag{38}$$

$$\theta_{sz} = \arctan\left(\frac{N_n}{M_n}\right)$$

where

$$M_n = \int_{X_1}^{X_2}\left(D_1\cos\tfrac{1}{2}\overline{X_b} - D_2\sin\tfrac{1}{2}\overline{X_b}\right)\phi_n X_b\, dX_b$$

$$N_n = \int_{X_1}^{X_2}\left(D_2\cos\tfrac{1}{2}\overline{X_b} + D_1\sin\tfrac{1}{2}\overline{X_b}\right)\phi_n X_b\, dX_b$$

$$D_1 = \frac{\sin\alpha_1 X_b^2}{6(2n+1)}\frac{\sin\tau}{\tau}$$

$$D_2 = \left(1 + \frac{3}{8}\right)\frac{\sin\tau}{\tau} - \frac{X_b^2\sin\alpha_1}{6(2n+1)}\left(\frac{\cos\tau}{\tau} - \frac{\sin\tau}{\tau^2}\right)$$

where $X_1 = \overline{X_b} - \delta\overline{X_b}$ and $X_2 = \overline{X_b} + \delta\overline{X_b}$.

Results

The results are presented in two parts. The first focuses on the relative magnitudes of $F_{pq}\phi_n$ which comprise the second-order forcing functions (29) and (37) from the offshore and surf zone regions, respectively. The second part compares initial growth rate amplitudes and phases in the two regions, (30) and (38), and for the total combined forcing. Sensitivity to mode number, n, and wave angle, $(\alpha_i)_o$, are examined in each part. Model parameters used in the following analysis are $\tan\beta = 0.01$, $\gamma = 0.42$, $\delta = 0.1$, and $x_b = 100$ m, chosen as reasonable for field situations. For convenience, incident wave angles were chosen to be identical at the breakpoint. Results are plotted against the nondimensional variable

$$\chi_b = \frac{\sigma_e^2 x_b}{g\tan\beta} \tag{39}$$

The range of values plotted, $\chi_b \le 10$, covers the range of typical infragravity frequencies commonly observed in nature.

Forcing Components

The relative strength of the components of $\mathbf{F}(a_1, a_2, x)\phi_n(x)$ for mode 0 edge waves by the offshore and surf zone mechanisms is shown in Figure 3. The magnitude and phase for the case of $(\alpha_1)_o = (\alpha_2)_o = 10°$ are plotted as a function of nondimensional χ_b (the legend defining individual forcing components is given in the figure caption). For small χ_b, F_{xx} dominates the forcing in each region. At higher χ_b, longshore fluxes become relatively more important. Because the forcing decays rapidly as χ_b increases (for mode 0), considering only F_{xx} gives a good first-order approximation to the overall forcing. The forcing at higher modes, $n = 1$, 2, and 3, is shown in Figure 4 for $(\alpha_1)_o = (\alpha_2)_o = 10°$. Only the forcing magnitudes are shown since the phases of F_{pq} are the same as for mode 0 (Figure 3). The behavior of the forcing is similar in each region, with F_{xx} dominating all modes due to the dependence of F_{xy} (and F_{yx}) on $(2n+1)^{-1}$ and F_{yy} on $(2n+1)^{-2}$. Since F_{xx} is insensitive to mode number, the forcing at higher modes will be nearly the same as for the low modes, suggesting that all modes should be about equally forced.

In general, the amplitude of the forcing function in the surf zone is an order of magnitude larger than in the offshore region. Thus it is expected that this part of the forcing will dominate the growth rate. Since the forcing function in the surf zone is nearly independent of χ_b (to first order), the

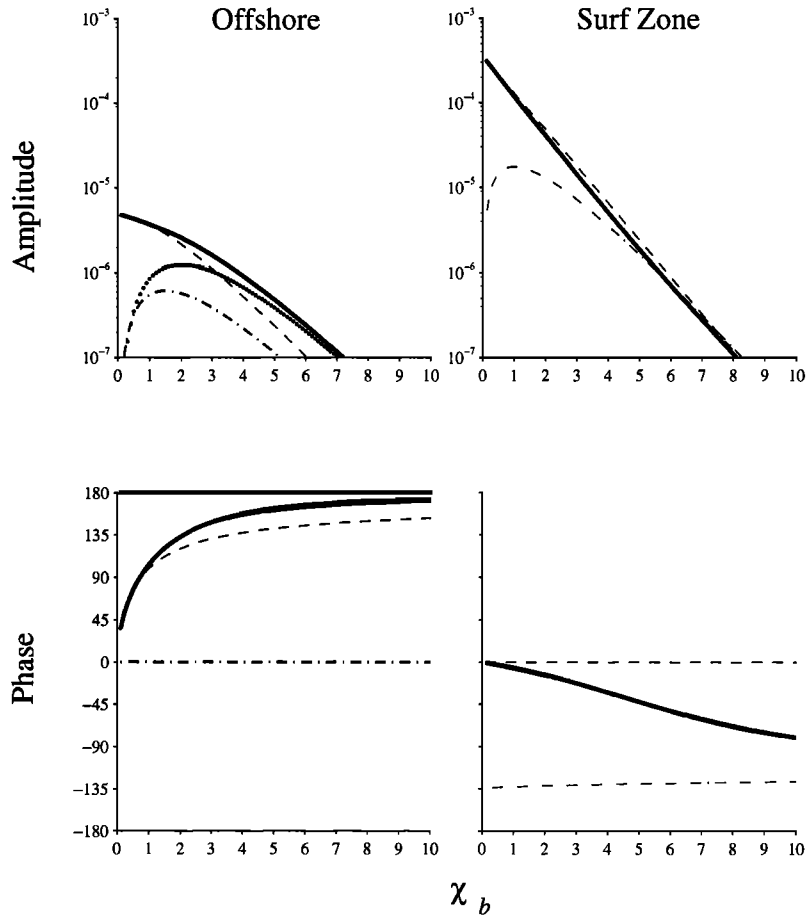

Figure 3. Contributions to the total edge wave forcing function, $\mathbf{F}\phi_n$, for a mode 0 edge wave, (left) from the offshore region and (right) within the surf zone. The components of the forcing arising from F_{xx} (dashed lines), F_{xy} (dash-dotted lines), F_{yy} (dotted lines), and the vector sums (solid lines) are plotted as a function of $\chi_b = \sigma_e^2 x_b / g\tan\beta$ (in the offshore region, $F_{yx} = F_{xy}$ so that $2F_{xy}$ is plotted, whereas in the surf zone, F_{yx} and F_{yy} are zero). Results are shown for $(\alpha_1)_o = (\alpha_2)_o = 10°$. Forcing amplitudes (m/s^2) on a log scale are shown in the top panels; forcing phase (degrees) on a linear scale is shown in the bottom panels. Results are computed for $\tan\beta = 0.01$, $\gamma = 0.42$, $\delta = 0.1$, and $x_b = 100$ m.

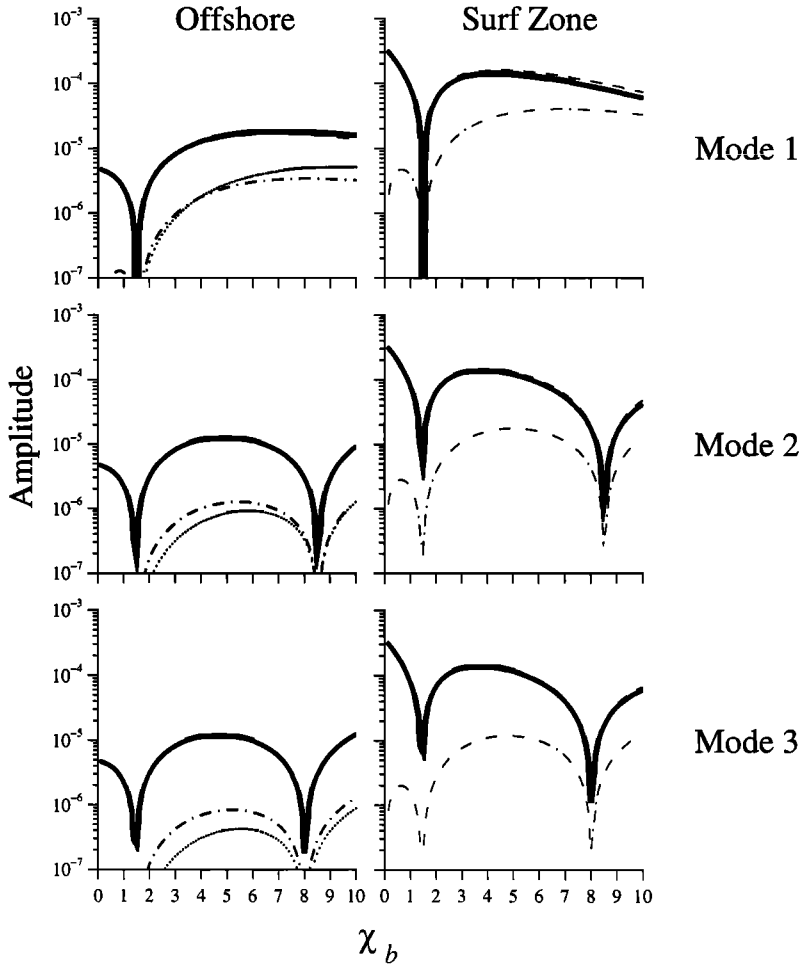

Figure 4. Forcing components arising from F_{xx} (dashed lines), F_{xy} (dash-dotted lines), F_{yy} (dotted lines), and the vector sum, $\mathbf{F}\phi_n$ (solid lines), for edge wave modes 1-3, with $(\alpha_1)_o = (\alpha_2)_o = 10°$, plotted as a function of $\chi_b = \sigma_e^2 x_b / g \tan\beta$. Contributions from the offshore and surf zone regions are shown in the left and right panels, respectively. Only the amplitudes are plotted since the component phases are identical to mode 0 (Figure 3; the total phase does vary slightly as a function of mode). Results are computed for $\tan\beta = 0.01$, $\gamma = 0.42$, $\delta = 0.1$, and $x_b = 100$ m.

spectral dependence of the forcing term will be determined by the form of the edge wave waveform, having nodes at particular χ_b. If the integration of the coupling occurs over a narrow range of χ_b, then the spectral shape of the ϕ_n will be strongly reflected in the growth rate.

The effect of $(\alpha_i)_o$ is examined in Figure 5 with $(\alpha_1)_o = (\alpha_2)_o = 1°$, 10°, and 30°. Results for a mode 1 edge wave are shown as a representative example. At small angles, F_{xx} dominates the forcing, being an order of magnitude greater than the other terms. However, the forcing for low modes should be enhanced for steeper angles of incidence because F_{xy} and F_{yy} have a strong modal and angular dependence, although on shallow beaches, incident wave angles are not expected to be large owing to refraction effects.

Growth Rates

Normalized growth rate magnitudes, G, and phases, θ, for the offshore and surf zone regions (equations (30) and (38)) and the total (vector sum) are shown in Figure 6 for edge wave modes 0-3 with $(\alpha_1)_o = (\alpha_2)_o = 10°$. The amplitudes are plotted on a log scale and the phases on a linear scale, as a function of χ_b. As expected, the growth rates within the surf zone region are much larger (by a factor of 2-10) than in the offshore region. The growth rates are rapid, with a magnitude of about 10^{-1} across most of the range of χ_b plotted. Because of the choice of normalization, the inverse of G gives the number of edge wave periods for the edge wave amplitude to grow to the size of the incident waves. Thus, assuming no dissipation, resonantly excited edge waves could grow to the same amplitude as the incident modulation in as fast as 10 edge wave periods (and even faster for lower modes and small χ_b). The model predicts only initial, undamped growth rates (essentially the rate at which energy is transferred from incident to edge waves), and any reasonable damping mechanism will reduce these rates. The effect of damping is discussed in the next section.

The results for the surf zone forcing mechanism show sharp valleys corresponding to nodes (zero crossings) in ϕ_n. The shape of the edge wave profiles is similar to the growth rates for the surf zone mechanism. The corresponding valley in the offshore growth rate does not occur at the first edge wave node ($\chi_b = 1.5$), nor is there any indication of strong nodal structure at higher χ_b. This result is due to integrating the

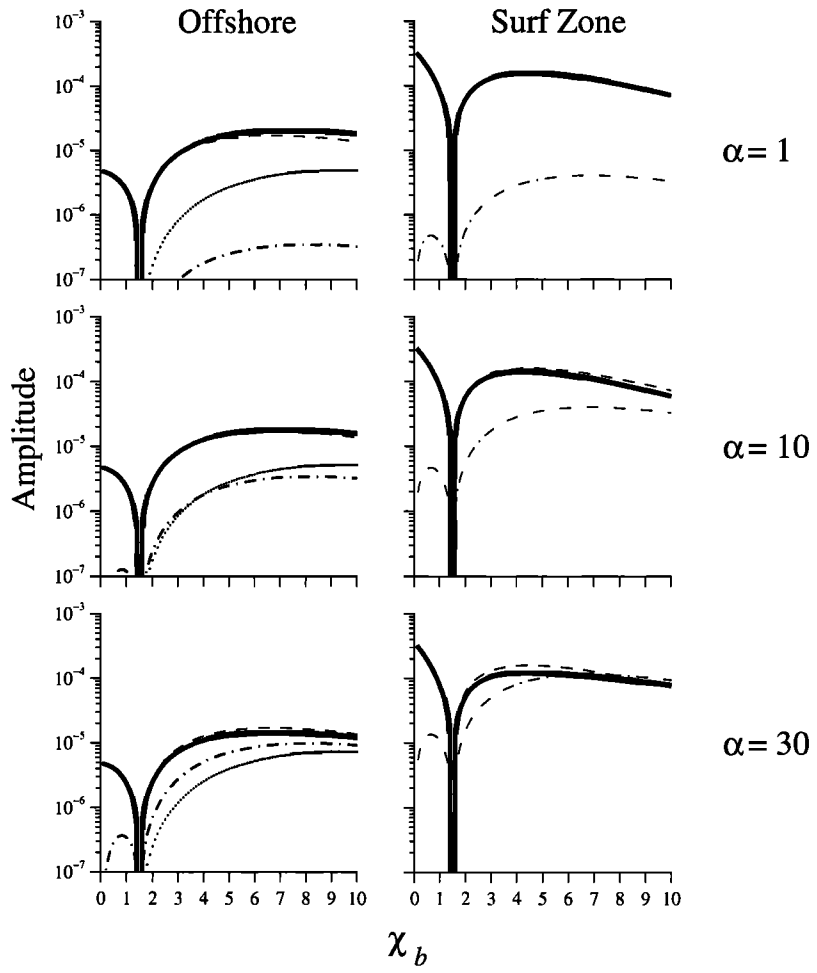

Figure 5. Effect of incident wave angle ($(\alpha_1)_o = (\alpha_2)_o = 1°$, 10°, and 30°) on the forcing components for a mode 1 edge wave. Format is the same as in Figure 4.

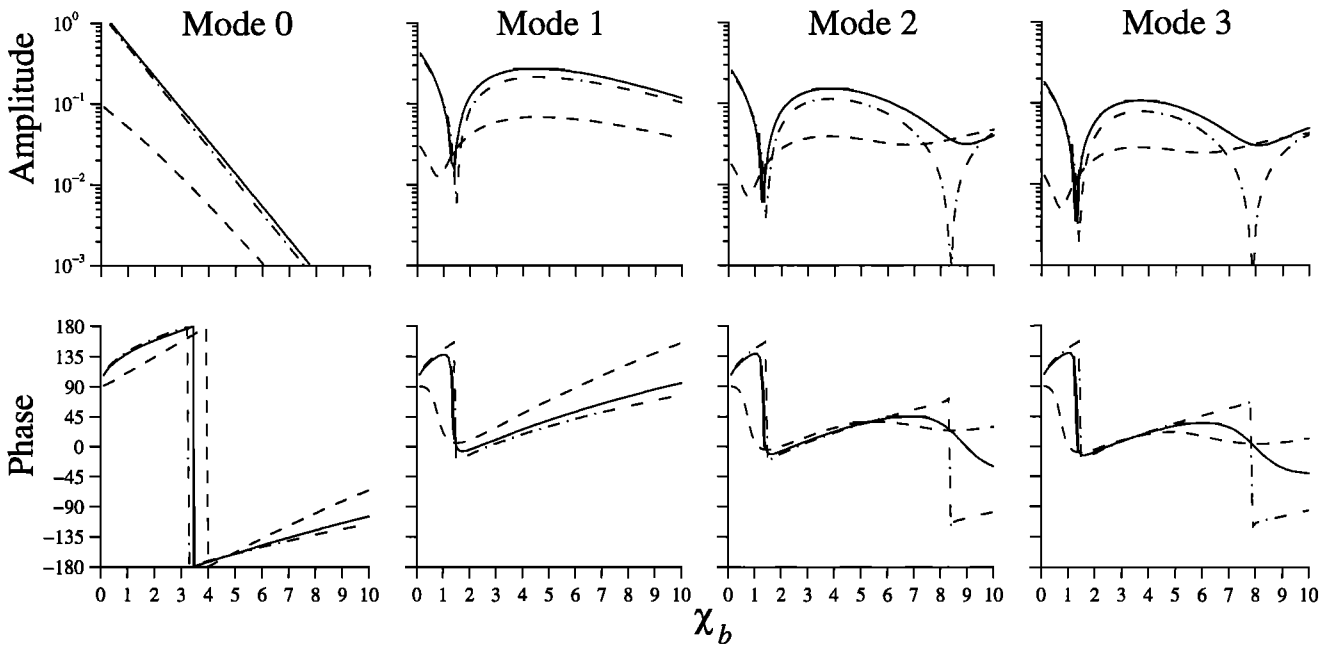

Figure 6. Normalized inviscid growth rate (top) magnitude and (bottom) phase for edge wave modes 0-3. Growth rates for the offshore region (dashed lines; (30)), the surf zone region (dash-dotted lines; (38)), and the total (solid lines), are shown as a function of $\chi_b = \sigma_e^2 x_b / g \tan\beta$. The inverse of the growth rate is the number of edge wave periods necessary for the edge waves to grow to the size of the incident waves. Results are shown for $(\alpha_1)_o = (\alpha_2)_o = 10°$, $\tan\beta = 0.01$, $\gamma = 0.42$, $\delta = 0.1$, and $x_b = 100$ m.

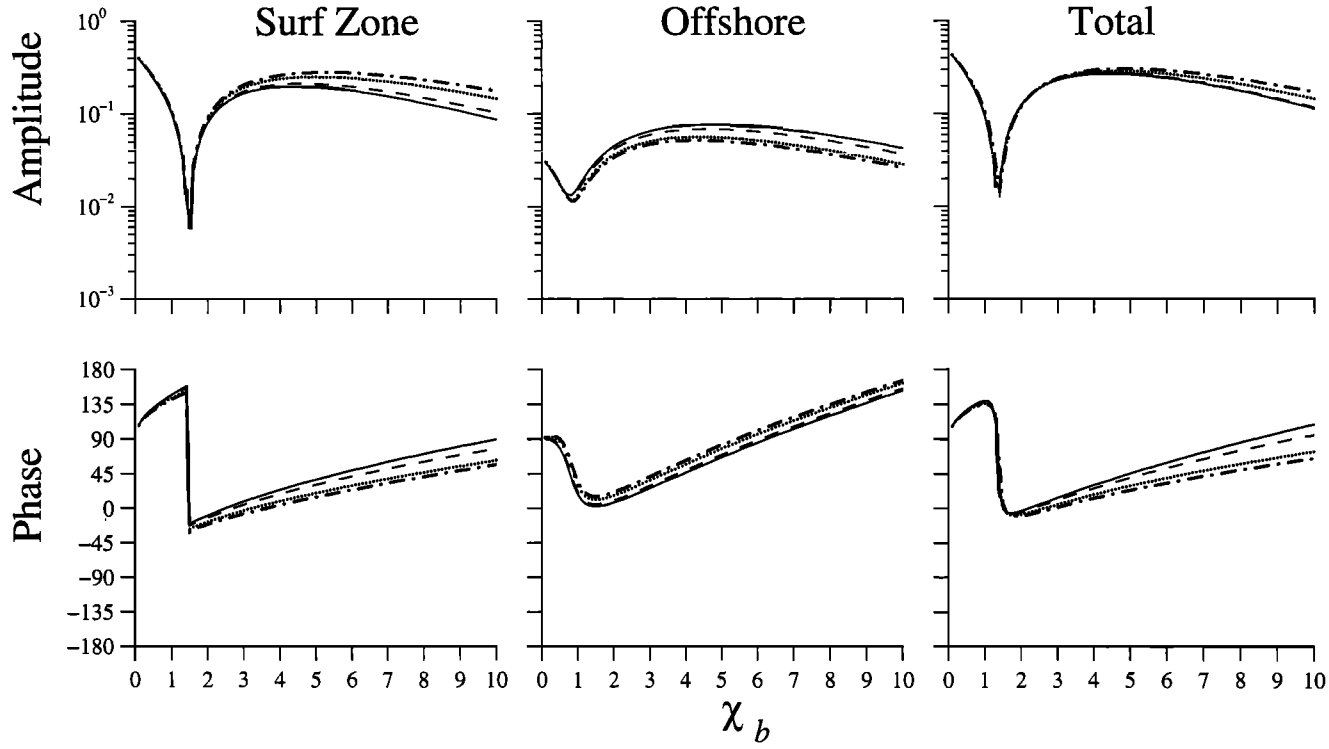

Figure 7. Effect of incident wave angle on inviscid growth rates for a mode 1 edge wave. Results are shown for (left) the surf zone, (middle) offshore, and (right) total for $(\alpha_1)_o = (\alpha_2)_o = 1°$ (solid lines), 10° (dashed lines), 30° (dotted lines), and 45° (dash-dotted lines). Format is the same as in Figure 6.

forcing in the offshore region over a larger length of the edge wave profile. In the surf zone, the length over which the forcing occurs is very much smaller, determined by the incident modulation ($\delta = 0.1$), and thus nodal points are strongly reflected in the growth rates.

The effect of α on growth rates is shown in Figure 7 for $n = 1$ with $(\alpha_1)_o = (\alpha_2)_o = 1°$, 10°, 30°, and 45°. The effect of α is small for the directional range investigated, particularly for the offshore region where $2F_{xy}$ and F_{yy} are π out of phase. The angular dependence is more pronounced in the surf zone region for $\chi_b > \sim 3.0$, increasing the growth rate about a factor of 2 from 1° to 45°. Interestingly, in the offshore region, increases in wave angle tend to reduce the growth rate (a consequence of the π phase relationships in the longshore components of F_{pq}), whereas the opposite occurs in the surf zone where the growth rate becomes larger as wave angle increases (owing to increased contributions from F_{xy}).

Discussion

Growth Rates

The predicted growth rates for the case of phase-locked forcing by deterministic wave trains are not unrealistic if we expect this mechanism to provide reasonable forcing of progressive edge waves under the stochastic forcing conditions found in nature [*Holman*, 1981]. The same type of result arose in the study of energy transfer into internal gravity waves from surface wave packets. An initial study of *Watson et al.* [1976] showed a very strong forcing for the phase-locked case. *Olbers and Herterich* [1979] redid the problem for a stochastic surface wave field and found the strength of the forcing to be several orders of magnitude weaker than predicted by Watson et al. This suggests that our predicted growth rates are higher than can be expected in nature and places an upper bound on edge wave growth

We have considered the forcing due to an interacting incident wave field consisting of only two shallow water waves, yet in natural situations, incident wave fields are distinctly not bichromatic but rather consist of a spectrum of energy. If we have a continuous directional spectrum in nature, some (small) components of the forcing will satisfy the resonance condition for a number of different edge waves of various frequencies and wavenumbers.

In the offshore region where we have referenced amplitudes to the breakpoint, the spectral problem seems inherently linear where the superposition of many wave components leads to the possibility of resonant triad interactions occurring for any number of different $(\sigma_i - \sigma_j, k_i - k_j)$ incident wave pairs. The forcing of a particular edge wave mode is just a linear sum of all possible interactions satisfying the edge wave dispersion relation. *Bowen and Guza* [1978] discuss the implications of this resonant restriction and show that for narrow-beam incident swells, some frequency selection, with a strong modal dependence, may be expected.

In the surf zone, the situation is more complicated because amplitudes are functions of local depth (and hence distance for monotonic beaches). However, for the bichromatic case, the forcing is dominated by F_{xx} arising from the self-self interaction of the primary wave. If we consider only this term, then the growth rate equation takes the form

$$\frac{1}{(a_i)_o f_e}\frac{\partial a_n}{\partial t} e^{-i\psi_e} = \frac{-2\pi i}{(a_i)_o g \tan\beta(2n+1)} \int_0^{x_b(y,t)} \overline{F}(x_b)\phi_n(x)dx \tag{40}$$

where $\overline{F}(x_b)$ is the mean forcing arising from $F_{xx}(\Phi_1\Phi_1)$. The operand of the coupling integral is simply a function of the edge wave waveform with amplitude equal to $\overline{F}$. The possibility of edge wave forcing arises if the temporal and spatial scales of the oscillating breaker line match the edge wave dispersion relation. For the spectral case, the breaker line is described by a summation of perturbations about a mean breakpoint. Edge wave forcing results from a linear combination of various incident wave pairs contributing to the alongshore perturbation, where the contribution from any particular pair (with amplitudes $a_1 a_2$) can be shown (Appendix B) to be

$$\Delta x_b = \frac{4}{H_o \gamma \tan\beta} a_1 a_2 \cos(\psi_1 - \psi_2) \tag{41}$$

where H_o is the mean breaker height calculated over all incident wave spectral components.

Since Δx_b is a function of y and t, the Fourier transform of (41) results in a spectral form for the perturbation, now given in terms of longshore wavenumber and frequency. This leads to the attractive result that time and space dependent observations of the width of the surf zone can be related to the edge wave forcing by the frequency-wavenumber spectrum of the wave breaking distribution.

As indicated by the growth rate equations (30) and (38), the behavior of the forcing as a function of the various parameters turns out to be quite simple. Growth rate contributions from the surf zone mechanism vary with χ_b in a way which largely follows the shape of ϕ_n. In the offshore region, the influence of mode number on actual rates is largely through the variance distribution of ϕ_n in χ_b space. That is, the rate of transferring energy from the incident field appears to be about the same for all modes, where, for higher modes, the energy must be spread over a larger cross-shore distance.

The only known measurements of growth rates for progressive edge waves are from the laboratory investigation of *Bowen and Guza* [1978]. Strict comparison with their results is difficult since their discussion was limited to $\chi_b \approx 0.25$, and furthermore, they have $\delta = 1.0$, thus violating our assumption of small-amplitude modulation. Their observed growth rate is over an order of magnitude slower than predicted by the model. The effect of viscous damping is likely to be important in the laboratory case, and since the scales of the lab study are much different from those typically found in nature, no simple comparison is readily made. In addition, any reasonable damping mechanism is likely to be different in the two forcing regions and may well have characteristics which lead to preferential damping of high frequencies and low modes [*Bowen and Guza*, 1978; *Holman*, 1981].

Damped Growth Rates

Up to this point we have considered only the undamped edge wave growth rate. Here we briefly examine the effect of frictional damping. If we retain the frictional term in (2) and (3), the normalized growth equation (11) takes the form

$$\left[(2\sigma_e + i\lambda)\frac{\partial a_n}{\partial t} + \lambda\sigma_e a_n\right]\frac{\pi e^{i\psi_e}}{(a_1)_o \sigma_e^2} = \frac{i2\pi}{(a_1)_o g \tan\beta(2n+1)}\int_0^\infty F\phi_n dx = G \tag{42}$$

where G is found from (30) and (38) for the two forcing regions. Taking the magnitude of the real part of (42) results in a quadratic equation in $\partial a_n/\partial t$ which has solution of the form

$$\frac{\partial a_n}{\partial t} = c_1 a_n[-1 \pm f(a_n)] \tag{43}$$

where

$$c_1 = \frac{2\lambda\sigma_e^2}{\lambda^2 + 4\sigma_e^2}$$

$$f(a_n) = \frac{1}{2\sigma_e}\sqrt{-\lambda^2 + \left(1 + \frac{4\sigma_e^2}{\lambda^2}\right)\frac{(a_1)_o^2 \sigma_e^2 |G|^2}{\pi^2 a_n^2}}$$

The case of interest is the positive root, corresponding to energy transfer from the incident waves to the edge waves. We have already assumed that the frictional dissipation has only a negligible effect on the wave solutions and dispersion relation; thus $\lambda^2 << 4\sigma_e^2$. Integrating (43) and considering only edge wave growth give a transcendental form for the amplitude

$$a_n = c_o e^{-c_1 t} e^{c_1 \int f(a_n) dt} \tag{44}$$

where c_o is an integration constant and for growth to occur $f(a_n)$ must be real and positive. This equation cannot be solved analytically; however, we can examine the amplitude decay (dissipation) when the forcing is turned off ($|G| = 0$) and the expected amplitude at equilibrium ($\partial a_n/\partial t = 0$).

For the case where the forcing is turned off, (44) becomes

$$\frac{a_n}{(a_n)_o} = e^{-\frac{1}{2}\lambda t} e^{i\frac{\lambda^2}{4\sigma_e}t} \qquad |G| = 0 \tag{45}$$

where $(a_n)_o$ is the initial edge wave amplitude at $t = 0$. Taking the magnitude of (45), the decay timescale normalized by the edge wave period is found

$$\frac{t}{T_e} = \frac{-2\ln[a_n/(a_n)_o]}{\lambda T_e} \tag{46}$$

It still remains to parameterize the damping. We take a very simple form for λ following *Longuet-Higgins* [1970]

$$\lambda = \frac{C_d |\mathbf{u}_0|}{h_0} \tag{47}$$

where h_0 is the depth at the breakpoint, C_d is a bottom drag coefficient of order 10^{-2}-10^{-3}, and u_0 is the magnitude of the linear orbital velocity of the incident wave of height H_0 at the breakpoint given by

$$\mathbf{u}_0 = \frac{1}{2}\left[\frac{\sqrt{\pi}}{2} H_0 \sqrt{\frac{g}{h_0}}\right] \tag{48}$$

Using $H_o = \gamma x_o \tan\beta$ gives

$$\frac{t}{T_e} = \frac{-4\ln[a_n/(a_n)_o]}{\gamma\pi^{3/2}}\left(\frac{\tan\beta}{C_d}\right)\chi_b^{1/2} \tag{49}$$

A plot of t/T_e as a function of χ_b for various values of $\tan\beta/C_d$ with $a_n/(a_n)_o = 0.5$ is shown in Figure 8. The half-

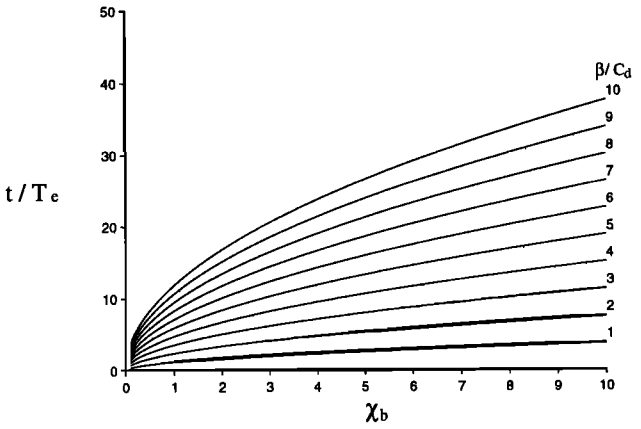

Figure 8. Normalized edge wave decay timescales (equation (49)) as a function of $\chi_b = \sigma_e^2 x_b / g \tan\beta$, for various values of $\tan\beta/C_d$. The vertical axis is in number of edge wave periods for the edge wave amplitude to decay 50% ($(a_n)/(a_n)_o = 0.5$) after the forcing is turned off. Results are shown for $\gamma = 0.42$.

life decay scale is moderately insensitive to χ_b. The ratio $\tan\beta/C_d$ is a rough indication of the Q (resonance) of the system, with higher values corresponding to weakly damped conditions with small drag coefficients. Steep beaches tend to have smaller dissipation rates than flat beaches, intuitively in agreement with conceptual damping mechanisms [*Bowen and Guza*, 1978; *Komar*, 1979; *Holman*, 1981]. For resonant systems, half-lives can be as high as 10-30 edge wave periods.

At equilibrium, we can estimate the size of edge wave amplitudes relative to incident waves from (42)

$$\frac{a_n}{(a_1)_o} = \frac{4|G|}{\gamma\pi^{3/2}}\left(\frac{\tan\beta}{C_d}\right)\chi_b^{1/2} \qquad \frac{\partial a_n}{\partial t} = 0 \qquad (50)$$

This form can also be obtained from the simple argument that $f(a_n)$ in (43) must be real for growth to occur. A plot of $a_n/(a_1)_o$ is shown in Figure 9 as a function of χ_b for various values of $\tan\beta/C_d$ and with $|G|$ estimated conservatively from Figures 6 and 7 to be about 0.05. *Guza and Thornton* [1982] found edge wave rms amplitudes in the run-up of a near planar beach as high as 75% of the incident wave rms amplitude. *Holman and Sallenger* [1985] also observed edge waves of this magnitude on a barred beach under a wide range of conditions. The model suggests amplitude ratios of this magnitude for $\tan\beta/C_d$ values ranging from 3 to 10. Comparison with field results is not strictly quantitative because waves in nature are never truly bichromatic, although it is noted that *Komar* [1979] suggested that $\tan\beta/C_d$ ratios of this magnitude are reasonable for mean currents on beaches often found in nature.

The damping parameterization used in (47) is only applicable to waves in the surf zone. It is not known what the damping mechanism is in the offshore region. *Herbers et al.* [1995a] show that the ratio of shoreward to seaward propagating free infragravity waves decreases as sea and swell energy increases, suggesting that the damping of edge waves on the shelf depends on the incident wave energy level, in qualitative agreement with the surf zone damping mechanism examined.

Sensitivity to Model Parameters

The dependence of growth rates on $\bar{x}_b$, $\tan\beta$, and σ_e is essentially combined into the nondimensional scaling parameter χ_b (equation (39)). Thus measured spectra obtained in the field can be interpreted in terms of sampling position and lowest-order profile characteristics. The effect of varying any particular combination of parameters is easily deduced. Additionally, because the forcing is dominated by F_{xx}, incident wave angles have little influence on the growth rate, except for low modes and large angles of incidence.

In the model, $\gamma = 0.42$ is assumed constant, consistent with field data [*Thornton and Guza*, 1982; *Sallenger and Holman*, 1985], and enters the growth rate equations (30) and (38) linearly. Since all reported values of γ are $O(1)$, varying γ is not expected to significantly influence the final results. Thus the formulation of the growth rate (in both the offshore and surf zone regions) is dependent on only one free parameter: the incident modulation, δ. Allowing the modulation to get much larger than about 0.1 is not accounted for exactly by the model, where we have assumed small δ, so that incident wave travel times are short compared to timescales associated with the modulation [*Symonds et al.*, 1982].

Since terms in the radiation stress containing Λ (equation (28)) are small compared to other terms, the forcing is effectively independent of incident frequencies. Hence the incident frequencies serve only to provide a necessary (σ_f, k_f) interaction which matches the edge wave dispersion relation. Products in incident wave velocity potentials, $\Phi_i\Phi_j$ (equation (23)), have an $(X_iX_j)^{-1/2}$ dependence, which contains products of incident frequencies $\sigma_i\sigma_j$. However, we have removed the dependence on incident frequencies in the formulation of $S(\Phi_i\Phi_j)$ by choosing incident wave amplitudes relative to the breakpoint, where products a_ia_j have an $(X_iX_j)^{1/2}$ dependence. Substituting (27) into (21) eliminates dependencies on $\sigma_i\sigma_j$.

Still, the resonant response assumed in the model restricts incident wave pairs to difference frequencies and wavenumbers which satisfy the edge wave dispersion relation. *Bowen and Guza* [1978] discuss these resonant restrictions in terms of incident wave angles and frequencies. They show that only a

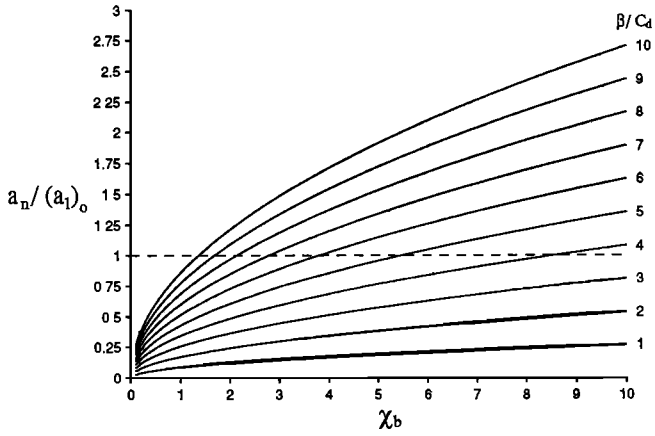

Figure 9. Normalized edge wave equilibrium amplitude (equation (50)) as a function of $\chi_b = \sigma_e^2 x_b / g \tan\beta$ for various values of $\tan\beta/C_d$. Edge wave amplitudes have been normalized by the incident wave amplitude at the breakpoint. Results are shown for $\gamma = 0.42$ and $|G| = 0.05$.

finite number of incident frequency pairs satisfy the resonant condition for a narrow beam incident swell. This places a restriction on the possible (σ_1, σ_2) combinations which could theoretically excite edge waves.

Shallow Water Assumption

In our formulation of the interaction radiation stress, the incident wave surface elevation is approximated by the shallow water Bessel function solution for progressive gravity waves over a sloping bottom. Inside the surf zone this formulation seems very reasonable since the water depth is always shallow with respect to incident wave wavelengths and amplitudes are given as a function of the local depth. Outside the surf zone, however, the use of the shallow water solution (which gives resonant triad interactions) is only valid for a limited distance offshore (determined by the beach slope) and depends on the incident wave frequency. In the offshore region, (24) gives an $x^{-1/4}$ dependence on wave amplitude. Thus products of incident wave amplitudes decay in this region as $x^{-1/2}$, whereas they should become constant in deep water where the wave profile we have assumed is only approximate. As there are no resonant triad interactions in deep water (only forced waves are generated), the magnitude of the forcing dies away quickly as incident waves approach deep water [*Okihiro et al.*, 1992].

The growth rate equation also includes consideration of ϕ_n. Since ϕ_n decays exponentially offshore as a function of mode number, the offshore integral for low modes is not biased significantly by reduced contributions in intermediate water. Therefore, when evaluating the model, the upper limit of integration can be reduced for low sloping beaches without substantially underestimating the growth rate. This approximation is good for shallow beaches where edge wave length scales are small; for steep beaches the application is questionable. The approximation is also more accurate for the case of low modes which have a relatively rapid offshore decay; for higher modes with slower decay scales, contributions are more severely biased.

Comparison With *Foda and Mei* [1981]

Foda and Mei [1981] consider the problem of long waves generated by a normally incident swell which has a small alongshore variation which is fixed in space but has a slow modulation in time. This variation in wave height could be thought of as two incident waves of the same frequency approaching the beach from equal, but opposite, angles to the normal. The modulation is then the beat frequency between these waves and the normally incident wave. This is therefore a rather particular case of the general problem which we are considering. Their discussion was further limited in that the dominant (largest) wave is normally incident. However, Foda and Mei have carried through a very sophisticated analysis which includes results for the case where the long waves grow to magnitudes of the same order as the incident modulation. They can therefore discuss the processes that eventually limit edge wave growth. However, the complexity of the calculation rather precludes any simple interpretation of these results.

A further complication is that, for the case of breaking waves, *Foda and Mei* [1981] have used a representation of the breaker condition in which the breakpoint is constant and the perturbation amplitude (modulation) extends to the shoreline; the variation in breaker position due to changing wave conditions is ignored. In effect, Foda and Mei assume that γ is always larger when the incident waves are large. Field evidence [*Guza and Thornton*, 1982; *Sallenger and Holman*, 1985] suggests that γ is reasonably constant for any particular beach and the position of the breaker is the property that varies as a function of incident wave height. This is a central point in our calculation.

Foda and Mei [1981] also compute growth rates for the interaction which vary over 2 orders of magnitude as a function of the parameter

$$\overline{\Omega} = \frac{\sigma_e}{\beta \sigma_i} \tag{51}$$

This parameter arises from a particular scaling which is not the natural scaling for the shallow water equations on a sloping beach we have considered (equation (39)). As a consequence, Foda and Mei have computed values of $\overline{\Omega}$ which are very small, ranging from 1 to 3. If we consider a 60*s* beat, 10*s* incident wave, and slope of 1:100, then $\overline{\Omega} \approx 16$. As growth rates increase very rapidly with $\overline{\Omega}$ in Foda and Mei's results, we might expect very large growth rates for values typical of open coast beaches. However, precise values cannot be compared due to their complex (fourth order) representation of the forcing inside the surf zone.

Conclusions

A theoretical mechanism for driving resonant edge waves in the nearshore is derived from the forced shallow water equations. Forcing integrals are separated into an offshore region outside the breakpoint and within the region of fluctuating surf zone width. Contributions to the surf zone region occur from primary self-self interactions for both breaking and nonbreaking waves, whereas in the offshore region, forcing is from cross interactions of a pair of waves. The strength of the forcing in each region is based on amplitude modulations which arise from an interacting bichromatic wave field. Surf zone forcing is derived from momentum fluxes induced by temporal and spatial variations in initial breakpoint amplitudes, expressed for the plane beach case as three-dimensional modulations in surf zone width (first suggested by *Symonds et al.* [1982] while focusing on the two-dimensional problem). The nonlinear forcing is provided by the unbalanced gradient in radiation stress, S_{pq}. Following *Phillips* [1977], a form for S_{pq} due to the nonlinear difference interaction of two incident waves approaching the beach at an angle is derived.

The model indicates that the forcing arising from the cross-shore component of onshore directed momentum flux provides the major contribution to the edge wave forcing, particularly for small angles of incidence, higher edge wave modes, and lower frequencies. Increasing incident wave angle tends to reduce the contribution in the offshore region for all modes because of the relative phase relationships of the forcing components, whereas the growth rate inside the surf zone is enhanced tending to favor the breakpoint mechanism in the overall growth rate.

We find that the strength of the surf zone generation mechanism is 2-10 times greater than in the offshore region for parameter ranges of particular interest. Thus considering only the surf zone component may provide a reasonable first-

order estimate of the growth rate. The strength of the growth rate is inversely proportional to edge wave mode number and directly proportional to the incident wave modulation, with a linear dependence in each region. Initial inviscid growth rates are found to be quite rapid, with edge waves amplitudes growing to incident wave amplitudes of the order of 10 edge wave periods.

Including a simple parameterization for bottom frictional damping and using inviscid growth rates to describe the energy transfer from incident to edge waves allow predictions of edge wave equilibrium amplitudes consistent with field measurements of *Guza and Thornton* [1982] and *Holman and Sallenger* [1985], who found shoreline amplitudes as high as 75% of the incident waves. Edge wave dissipation rates in the surf zone are found when the forcing is turned off and suggest half-life decay scales of the order of 10-30 edge wave periods for $\tan\beta/C_d$ values of about 3-10 (estimated from equilibrium conditions). Dissipation rates outside the surf zone are not estimated since the appropriate damping mechanism in this region is not known.

The extension to spectral forcing is shown to be possible. The development in the offshore region can be based on a linear sum of all possible combinations of wave triads satisfying the edge wave dispersion relation. The same is true for the surf zone, where the combination of various incident wave pairs contributes to the alongshore perturbation of the oscillatory breaker line. The contribution to spectral forcing by any particular pair is shown in principal to be due to the linear sum of all resonant interactions.

Appendix A: Expansion of First-Order Coupling Integrals

Edge wave growth rates are given as a function of the coupling integral between the wave forcing, **F**, and the edge wave waveform, ϕ_n

$$\frac{\partial a_n}{\partial t} \sim \int_0^\infty \mathbf{F}(\Phi_1, \Phi_2, x)\phi_n(x)dx \qquad \text{(A1)}$$

where Φ_1 and Φ_2 are velocity potentials of the incident waves which have amplitudes a_1 and $a_2 = \delta a_1$, respectively. The coupling integral can be separated at the breakpoint, $x_b(y, t)$, into surf zone (first term on right-hand side of (A2)) and offshore (second term on right-hand side of (A2)) integrals with the forcing defined in each region by $\mathbf{F}_{sz}$ and $\mathbf{F}_{off}$, respectively,

$$\int_0^\infty \mathbf{F}\phi_n dx = \int_0^{\bar{x}_b(1+\delta\cos\psi_e)} \mathbf{F}_{sz}\phi_n dx + \int_{\bar{x}_b(1+\delta\cos\psi_e)}^\infty \mathbf{F}_{off}\phi_n dx \qquad \text{(A2)}$$

where the breakpoint has been defined by $x_b(y, t) = \bar{x}_b(1+\delta\cos\psi_e)$ and the functional dependencies have been dropped for brevity.

The surf zone integral (first term on right-hand side) in (A2) can be further separated by the mean breakpoint, $\bar{x}_b$, into a nonvarying component from the shoreline to $\bar{x}_b$ and a component arising from modulations in the breakpoint position

$$\int_0^{\bar{x}_b(1+\delta\cos\psi_e)} \mathbf{F}_{sz}\phi_n dx = \int_0^{\bar{x}_b} \mathbf{F}_{sz}\phi_n dx + \int_{\bar{x}_b}^{\bar{x}_b(1+\delta\cos\psi_e)} \mathbf{F}_{sz}\phi_n dx \qquad \text{(A3)}$$

The first integral on the right-hand side of (A3) is zero since radiation stress gradients are constant inside the mean breakpoint. Thus, after evaluating the second integral in (A3)

$$\int_0^{\bar{x}_b(1+\delta\cos\psi_e)} \mathbf{F}_{sz}\phi_n dx = Q(\bar{x}_b + \delta\bar{x}_b\cos\psi_e) - Q(\bar{x}_b) \qquad \text{(A4)}$$

where $Q(x)$ is the unspecified result of the integration. Expanding (A4) in a Taylor's Series about $\bar{x}_b$ produces

$$\int_0^{\bar{x}_b(1+\delta\cos\psi_e)} \mathbf{F}_{sz}\phi_n dx = \delta\bar{x}_b\cos\psi_e \frac{\partial Q(\bar{x}_b)}{\partial x} + \frac{(\delta\bar{x}_b\cos\psi_e)^2}{2}\frac{\partial^2 Q(\bar{x}_b)}{\partial x^2} + \ldots \qquad \text{(A5)}$$

which can be written in terms of the integrand of (first term on right-hand side of (A2)) evaluated at $\bar{x}_b$ plus higher order harmonics

$$\int_0^{\bar{x}_b(1+\delta\cos\psi_e)} \mathbf{F}_{sz}\phi_n dx = \delta\bar{x}_b\cos\psi_e \mathbf{F}_{sz}(\bar{x}_b)\phi_n(\bar{x}_b) + O(\delta^2\cos 2\psi_e) + \ldots \qquad \text{(A6)}$$

Thus for the first integral on right-hand side of (A2) we need only consider the forcing at the mean breakpoint, $\mathbf{F}_{sz}(\bar{x}_b)$, which has terms arising from self and cross interactions of Φ_1 and Φ_2. The $\Phi_1\Phi_1$ and $\Phi_2\Phi_2$ interactions produce coupling terms which contain primary modulations ($\cos\psi_e$) of order δ and δ^3, respectively, whereas $\Phi_1\Phi_2$ interactions produce additional harmonic terms ($\cos 2\psi_e$) of order δ^2. Considering only first-order, primary modulations (arising from $\Phi_1\Phi_1$ interactions), the surf zone coupling integral is approximated by

$$\int_0^{\bar{x}_b(1+\delta\cos\psi_e)} \mathbf{F}_{sz}\phi_n dx = \delta\bar{x}_b\cos\psi_e \mathbf{F}_{sz}(\phi_1\phi_1, \bar{x}_b)\phi_n(\bar{x}_b) \qquad \text{(A7)}$$

As in the surf zone region, the offshore coupling integral (second term on right-hand side of (A2)) can be separated at $\bar{x}_b$,

$$\int_{\bar{x}_b(1+\delta\cos\psi_e)}^\infty \mathbf{F}_{off}\phi_n dx = \int_{\bar{x}_b(1+\delta\cos\psi_e)}^{\bar{x}_b} \mathbf{F}_{off}\phi_n dx + \int_{\bar{x}_b}^\infty \mathbf{F}_{off}\phi_n dx \qquad \text{(A8)}$$

The second integral on the right-hand side of (A8) has modulations which arise from only the $\Phi_1\Phi_2$ interactions and is numerically evaluated in the main text ($\Phi_1\Phi_1$ and $\Phi_2\Phi_2$ interactions produce only nonvarying components through this integral). The first integral describes the contribution to edge wave growth by nonbreaking waves in the fluctuating region of the surf zone. Evaluating this integral produces

$$\int_{\bar{x}_b(1+\delta\cos\psi_e)}^\infty \mathbf{F}_{off}\phi_n dx = R(\bar{x}_b) - R(\bar{x}_b + \delta\bar{x}_b\cos\psi_e) + \int_{\bar{x}_b}^\infty F_{off}(\Phi_1\Phi_2, x)\phi_n(x)dx \qquad \text{(A9)}$$

where $R(x)$ is the unspecified result of the integration. Expanding in a Taylor's series about $\bar{x}_b$ and keeping only first-order, primary modulations give

$$\int_{\bar{x}_b(1+\delta\cos\psi_e)}^{\infty} \mathbf{F}_{off}\phi_n dx = -\delta\bar{x}_b\cos\psi_e \mathbf{F}_{off}(\Phi_1\Phi_1, \bar{x}_b)\phi_n(\bar{x}_b) + \int_{\bar{x}_b}^{\infty} F_{off}(\Phi_1\Phi_2, x)\phi_n(x)dx \quad \text{(A10)}$$

The total coupling integral (A2) can thus be approximated

$$\int_0^{\infty} \mathbf{F}\phi_n dx = \delta\bar{x}_b\cos\psi_e\phi_n(\bar{x}_b)\left[\mathbf{F}_{sz}(\Phi_1\Phi_1, \bar{x}_b) - \mathbf{F}_{off}(\Phi_1\Phi_1, \bar{x}_b)\right] + \int_{\bar{x}_b}^{\infty} F_{off}(\Phi_1\Phi_2, x)\phi_n(x)dx \quad \text{(A11)}$$

which shows the first-order contributions to edge wave growth occur through self-self interactions from both breaking and nonbreaking waves within the fluctuating region of surf zone width, and through cross interactions of a pair of waves seaward of the average breakpoint position. Since the signs of $\mathbf{F}_{sz}$ and $\mathbf{F}_{off}$ are opposite in the fluctuating region of surf zone width, the $\Phi_1\Phi_1$ forcing contributions from breaking and nonbreaking waves reinforce.

Appendix B: Breakpoint Forcing in a Wave Spectrum

If the sea surface elevation η is described by

$$\eta = \sum_i a_i(x)\cos\psi_i \quad \text{(B1)}$$

where $\psi_i = l_i x + k_i y - \sigma_i t + \phi_i$, then the significant wave height is 4 times the standard deviation of η, and the mean wave height H_o is given by

$$H_o(x) = 2\left[\sum_i a_i^2\right]^{1/2} \quad \text{(B2)}$$

The variation in wave height, given by the envelope of the wave groups, can be defined and is often calculated in terms of the low-passed values of the square of the surface elevation, where

$$H(x,t) = 2\sqrt{2}\left[\langle\eta^2\rangle\right]^{1/2} \quad \text{(B3)}$$

where $\langle\ \rangle$ is the low-passed value; then from (B1),

$$\langle\eta^2\rangle = \left\langle \sum_i\sum_j \frac{a_i^2}{2}\left[1+\cos(2\psi_i)\right] + a_i a_j\left[\cos(\psi_i+\psi_j)+\cos(\psi_i-\psi_j)\right]\right\rangle \quad \text{(B4)}$$

the low-pass filter removes the high harmonics and sum interactions, so that

$$H(x,t) = 2\sqrt{2}\left[\sum_i \frac{a_i^2}{2} + \sum_i\sum_j a_i a_j\cos(\psi_i-\psi_j)\right]^{1/2} \quad \text{(B5)}$$

and the second term represents the perturbation of the wave height about its mean value.

The problem can be simplified if the perturbation of the wave height about the mean value H_o is not too large (it is, of course, necessarily less than one). So expanding (B5),

$$H(x,t) = 2\sqrt{2}\left[\sum_i \frac{a_i^2}{2}\right]^{1/2}\left[1+\frac{\sum_i\sum_j a_i a_j\cos(\psi_i-\psi_j)}{\sum_i a_i^2} + O\left[\cos^2(\psi_i-\psi_j)\right]\right] \cong H_o(x)\left[1+\frac{\sum_i\sum_j a_i a_j\cos(\psi_i-\psi_j)}{\sum_i a_i^2}\right] \quad \text{(B6)}$$

There is a potential forcing term for edge waves from each of the second terms in the expansion

$$\cos(\psi_i-\psi_j) = \cos\left[(l_i-l_j)x + (k_i-k_j)y - (\sigma_i-\sigma_j)t + \phi_i - \phi_j\right] \quad \text{(B7)}$$

with resonant forcing possible if

$$k_i - k_j = k_e \text{ and } \sigma_i - \sigma_j = \sigma_e \quad \text{(B8)}$$

where (σ_e, k_e) satisfy the edge wave dispersion relation. Within the spectra, the interaction between several different sets of incident waves can produce the same values of (σ_e, k_e), and the net forcing is the sum of all these potential inputs.

Now the wave breaks when $H = \gamma h$, so the mean breaker position h_b is given by

$$h_b = H_o(x_b)/\gamma \quad \text{(B9)}$$

and for a plane beach, the mean breakpoint is $x_b = H_o(x_b)/(\gamma\tan\beta)$. The perturbation in breaker height then leads to a variable breakpoint position in both the longshore direction and in time, where

$$x_b(y,t) = \frac{1}{\gamma\tan\beta}H(x,t) = \frac{H_o}{\gamma\tan\beta}\left[1+\frac{\sum_i\sum_j a_i a_j\cos(\psi_i-\psi_j)}{\sum_i a_i^2}\right] \quad \text{(B10)}$$

which is a linear combination of a large number of contributions to the longshore perturbation from pairs of incident waves. The contribution from any particular pair is then

$$\Delta x_b = \frac{4}{H_o\gamma\tan\beta}a_1 a_2\cos(\psi_1-\psi_2) \quad \text{(B11)}$$

Acknowledgments. This research was sponsored by the National Science Foundation under contract OCE-8007972-01 and by the Office of Naval Research under grant N00014-90-J1118. This work was completed while T.C.L was supported by a National Research Council Postdoctoral Fellowship. We thank Bob Guza and the reviewers for

their insightful comments which led to a correction to the surf zone forcing mechanism and in general greatly improved the paper. Joan Semler prepared the typeset manuscript.

References

Biesel, F., Equations generales au second ordre de la houle irreguliere, *Houille Blanche*, *7*, 372-376, 1952.

Bowen, A. J., and R. T. Guza, Edge waves and surf beat, *J. Geophys. Res.*, *83*C4), 1913-1920, 1978.

Eckart, C., Surface waves on water of variable depth, *Wave Rep. 100*, Scripps Inst. of Oceanogr., Univ. of Calif., La Jolla, 1951.

Foda, M. A., and C. C. Mei, Nonlinear excitation of long-trapped waves by a group of short swells, *J. Fluid Mech.*, *111*, 319-345, 1981.

Gallagher, B., Generation of surf beat by nonlinear wave interactions, *J. Fluid Mech.*, *49*, 1-20, 1971.

Guza, R. T., and A. J. Bowen, The resonant instabilities of long waves obliquely incident on a beach, *J. Geophys. Res.*, *80*(33), 4529-4534, 1975.

Guza, R. T., and E. B. Thornton, Swash oscillations on a natural beach, *J. Geophys. Res.*, *87*(C1), 483-491, 1982.

Guza, R. T., and E. B. Thornton, Observations of surf beat, *J. Geophys. Res.*, *90*(C2), 3161-3172, 1985.

Hasselmann, K., On the non-linear energy transfer in a gravity-wave spectrum, 1, General theory, *J. Fluid Mech.*, *12*, 481-500, 1962.

Herbers, T. H. C., S. Elgar, and R. T. Guza, Generation and propagation of infragravity waves, *J. Geophys. Res.*, *100*(C12), 24,863-24,872, 1995a.

Herbers, T. H. C., S. Elgar, R. T. Guza, and W. C. O'Reilly, Infragravity-frequency (0.005-0.05 Hz) motions on the shelf, II, Free waves, *J. Phys. Oceanogr*, *25*(6), 1063-1079, 1995b.

Holman, R. A., Infragravity energy in the surf zone, *J. Geophys. Res.*, *86*(C7), 6442-6450, 1981.

Holman, R. A., and A. H. Sallenger, Setup and swash on a natural beach, *J. Geophys. Res.*, *90*(C1), 945-953, 1985.

Howd, P. A., J. M. Oltman-Shay, and R. A. Holman, Wave variance partitioning in the trough of a barred beach, *J. Geophys. Res.*, 96(C7), 12,781-12,795, 1991.

Huntley, D. A., Long-period waves on a natural beach, *J. Geophys. Res.*, *81*(36), 6441-6449, 1976.

Huntley, D. A., R. T. Guza, and E. B. Thornton, Field observations of surf beat, 1, Progressive edge waves, *J. Geophys. Res.*, *86*(C7),. 6451-6466, 1981.

Komar, P. D., Beach-slope dependence of longshore currents, *J. Waterw. Port Coastal Ocean Div. Am. Soc. Civ. Eng.*, *105*(WW4), 460-464, 1979.

List, J. H., A model for the generation of two-dimensional surf beat, *J. Geophys. Res.*, *97*(C7), 5623-5635, 1992.

Longuet-Higgins, M. S., Longshore currents generated by obliquely incident sea waves, 2, *J. Geophys. Res.*, *75*(33), 6790-6801, 1970.

Longuet-Higgins, M. S., and R. W. Stewart, Radiation stresses and mass transport in gravity waves, with application to 'surf beats,' *J. Fluid Mech.*, *13*, 481-504, 1962.

Longuet-Higgins, M. S., and R. W. Stewart, Radiation stresses in water waves: A physical discussion, with applications, *Deep Sea Res.*, *11*, 529-562, 1964.

Mei, C. C., and C. Benmoussa, Long waves induced by short-wave groups over an uneven bottom, *J. Fluid Mech.*, *139*, 219-235, 1984.

Munk, W. H., Surf beats, *Eos Trans. AGU*, *30*(6), 849-854, 1949.

Okihiro, M., R. T. Guza, and R. J. Seymour, Bound infragravity waves, *J. Geophys. Res.*, *97*(C7), 11,453-11,469, 1992.

Olbers, D. J., and K. Herterich, The spectral energy transfer from surface waves to internal waves, *J. Fluid Mech.*, *92*, 349-379, 1979.

Oltman-Shay, J. M., and R. T. Guza, Infragravity edge wave observations on two California beaches, *J. Phys. Oceanogr.*, *17*(5), 644-663, 1987.

Phillips, O. M., *The Dynamics of the Upper Ocean*, 2nd ed., 336 pp., Cambridge Univ. Press., New York, 1977.

Sallenger, A. H., and R. A. Holman, Wave energy saturation on a natural beach of variable slope, *J. Geophys. Res.*, *90*(C6), 11,939-11,944, 1985.

Sallenger, A. H., and R. A. Holman, Infragravity waves over a natural barred profile, *J. Geophys. Res.*, *92*(C9), 9531-9540, 1987.

Schaffer, H. A., Infragravity waves induced by short-wave groups, *J. Fluid Mech.*, *247*, 551-588, 1993.

Schaffer, H. A., Edge waves forced by short-wave groups, *J. Fluid Mech.*, *259*, 125-148, 1994.

Schaffer, H. A., and I. Svendsen, Surf beat generation on a mild-slope beach, in *Proceedings of the 21st International Conference on Coastal Engineering*, pp. 1058-1072, Am. Soc. Civ. Eng., New York, 1988.

Stoker, J. J., Surface waves in water of variable depth, *Q. App. Math.*, *5*(1), 1-54, 1947.

Symonds, G., and A. J. Bowen, Interactions of nearshore bars with incoming wave groups, *J. Geophys. Res.*, *89*(C2), 1953-1959, 1984.

Symonds, G., D. A. Huntley, and A. J. Bowen, Two-dimensional surf beat: Long wave generation by a time-varying breakpoint, *J. Geophys. Res.*, *87*(C1), 492-498, 1982.

Thornton, E. B., and R. T. Guza, Energy saturation and phase speeds measured on a natural beach, *J. Geophys. Res.*, *87*(C12), 9499-9508, 1982.

Tucker, M. J., Surf beats: Sea waves of 1 to 5 minute period, *Proc. R. Soc. London A*, *202*, 565-573, 1950.

Watson, K. M., B. J. West, and B. I. Cohen, Coupling of surface and internal gravity waves: A mode coupling model, *J. Fluid Mech.*, *77*, 105-208, 1976.

A. J. Bowen, Department of Oceanography, Dalhousie University, Halifax, Nova Scotia, Canada B3H 461.

R. A. Holman, College of Ocean and Atmospheric Sciences, Oregon State University, OC Administration Building 104, Corvallis, OR 97331-5503.

T. C. Lippmann, Center for Coastal Studies, Scripps Institution of Oceanography, University of California, San Diego, 9500 Gilman Drive, La Jolla, CA 92093-0209, (e-mail: tlippmann@ucsd.edu.

(Received January 5, 1994; revised June 24, 1996;
accepted September 27, 1996.)